encit 2020

ABCM Associação Brasileira de Engenharia e Ciências Mecânicas

18th Brazilian Congress of Thermal Sciences and Engineering
November 16–20, 2020 (Online)

ENC-2020-0622
IMPROVED ANISOTROPIC TRANSPORT THROUGH POLYMER LAYER AND POROUS ARTERIAL WALL WITH BINDING IN DRUG-ELUTING STENTS

Fabiane Frazzoli
Haroldo Rosman
Rachel Lucena
Norberto Mangiavacchi
José Pontes
State University of Rio de Janeiro, Rio de Janeiro, RJ, Brazil
frazzoli.fabi@gmail.com, haroldo.rrj@gmail.com, rachel.lucena@gmail.com, norberto@uerj.br, jose.pontes@uerj.br
Gustavo R. Anjos
COPPE/Federal University of Rio de Janeiro, Department of Mechanical Engineering, Rio de Janeiro - Brazil
gustavo.rabello@coppe.ufrj.br
Sean McGinty
Division of Biomedical Engineering, University of Glasgow, Glasgow, UK
sean.mcginty@glasgow.ac.uk

Abstract. *Dissolution in the polymer coating and specific binding in the artery wall play an important role in anisotropic transport of the antiproliferative/anti-inflammatory drugs. In this work, we consider the model of dissolution, transport and binding of sirolimus on an axisymmetric domain representing the polymer coating layer and the porous artery wall in the vicinity of a stent strut. The Finite Element Method (FEM) is used to discretize the porous media equations by an interconnected unstructured triangular mesh and an improved anistropic model is employed to accurately capture the correct effect of the diffusion tension seem in the sirolimus concentration distribution. Finally, we present the new results obtained to the characterization of the dynamics of the porous arterial wall with binding in drug-eluting stents.*

Keywords: *drug-eluting stents, Darcy's law, convection-diffusion-reaction equations, anisotropic diffusion, finite element method*

1. INTRODUCTION

Drug-eluting stents (DES) marked a technology breakthrough in the field of percutaneous coronary intervention (PCI) due to a profound reduction in neointimal hyperplasia and the need for repeat revascularization as compared with bare-metal stents (BMS). However several concerns related to a higher risk of late thrombotic events and catch-up in efficacy during long-term follow-up hampered their widespread adoption in clinical practice, according to Chisari *et al.* (2016).

In DES, safety and efficacy are strongly influenced by the anisotropic transport of the antiproliferative/anti-inflammatory drugs in the arterial wall. Dissolution in the polymer coating and specific binding in the artery wall play an important role in the process. We developed a computational model employing the FEM on an unstructured mesh to discretise the governing equations. We consider the model of dissolution, transport and binding of sirolimus on an axisymmetric domain representing the polymer coating layer and the porous artery wall in the vicinity of a stent strut. We employ a nonlinear dissolution model for the dynamics of sirolimus in the polymer coating, and a nonlinear saturable binding model that includes both specific and non-specific binding in the arterial wall as separate phases, as proposed by McGinty and Pontrelli (2016). The arterial wall is considered an anisotropic porous media, and the flow is considered to be governed by Darcy flow. We consider the effect of the variation of the polymer properties, to show that the time evolution of the process can be efficiently controlled by the polymer diffusion coefficient.

The anisotropy in drug transport parameters, and in particular the diffusion tensor, is related to tissue fibres orientation. In a previous work (Frazzoli *et al.* (2018)) the diffusion tensor in the artery wall was considered orthotropic, with principal directions aligned with longitudinal (larger diffusion eigenvalue) and radial (smaller diffusion eigenvalue) directions, due to the orientation of tissue fibers in the artery wall, particularly plain muscle fibers in fine bundles, arranged in lamellae and disposed circularly around the vessel.

However, the presence of the stent causes the compression and realignment of tissue fibers, such that they are parallel to the stent surface in its proximity. Hence, the principal directions of the diffusion tensor must be re-oriented in the

vicinity of the stent to properly account for this stent-artery interaction.

In this work, the diffusion tensor is considered to be a general symmetric positive definite tensor, obtained by similarity transformation, considering the realignment of the principal directions obtained by an algebraic approach.

2. THE MATHEMATICAL MODEL AND NUMERICAL METHOD

In this work we assume a geometric symmetry about a reference axis, and therefore we employ an axisymmetric formulation. Figure 1(a) shows the model geometry where z direction is the axis of symmetry and r is the radial direction. The region Ω_1 represents the polymer layer and Ω_2 represents the arterial wall. An example of a bidimensional unstructured triangular mesh employed in the simulations is shown in Figure 1(b). The mesh was produced employing Gmsh mesh generator.

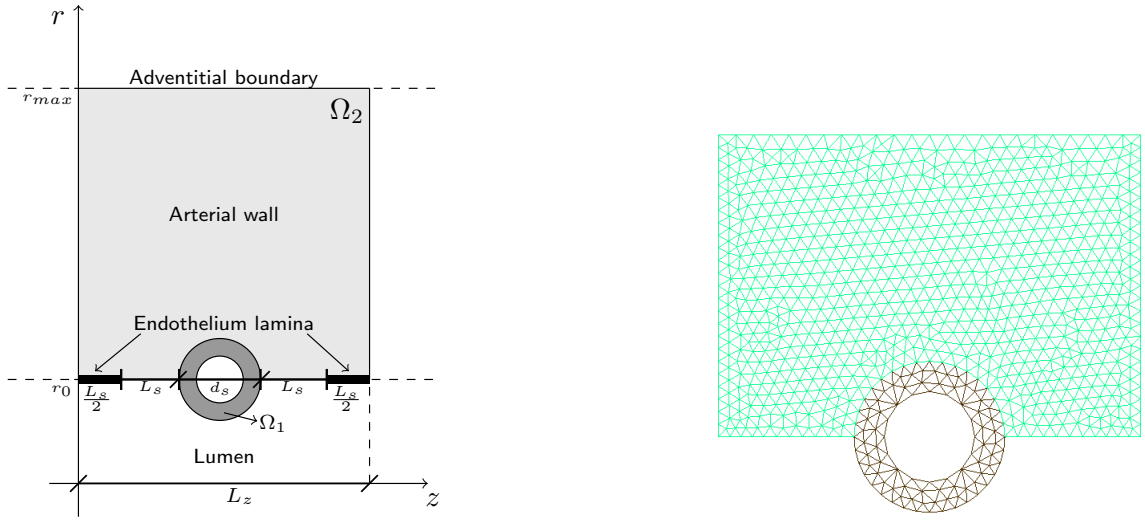

(a) (b)

Figure 1: (a) Model 2D axisymmetric geometry. Note that the endothelium is assumed to be denuded in the vicinity of the stent strut. (b) Computational domain and unstructured triangular mesh employed in the simulations. Black: polymer layer Ω_1. Green: arterial wall Ω_2.

We adopt the modeling framework of McGinty and Pontrelli (2016) and Bozsak *et al.* (2014). The arterial wall and the polymer layer are considered as porous media, and flow within these layers is assumed to be incompressbile and governed by Darcy's law:

$$\mathbf{u} = -\kappa_i \nabla p, \tag{1}$$

thus

$$\nabla \cdot (-\kappa_i \nabla p) = 0, \tag{2}$$

where $\mathbf{u} = (u, v)$ is the velocity field, p is the pressure in the arterial wall, $\kappa_i = P_{Di}/\mu$, P_{Di} is the Darcy permeability of the media and μ is the fluid viscosity.

The drug dynamics in the coating is modeled in terms of b_0 (solid) and c_0 (dissolved) concentrations by the equations:

$$\frac{\partial b_0}{\partial t} = -\beta_0 b_0^{2/3}(S_0 - c_0) \tag{3}$$

$$\frac{\partial c_0}{\partial t} + \mathbf{u}_s \cdot \nabla c_0 = \nabla \cdot (\mathcal{D}_0 \nabla c_0) + \beta_0 b_0^{2/3}(S_0 - c_0), \tag{4}$$

where $\mathbf{u}_s = \mathbf{u}/\phi_i$ is the seepage velocity, and ϕ_i is the effective porosity of the media, $\mathcal{D}_0$ is the effective scalar diffusion coefficient of the solute, β_0 the dissolution rate and S_0 is the solubility limit.

Drug elution in the arterial wall is governed by the convection-diffusion-reaction equations:

$$\frac{\partial c_1}{\partial t} + \mathbf{u}_s \cdot \nabla c_1 = \nabla \cdot (\mathcal{D}_1 \nabla c_1) - k_1^f c_1 (b_1^{max} - b_1) + k_1^r b_1 - k_2^f c_1 (b_2^{max} - b_2) + k_2^r b_2 \quad (5)$$

$$\frac{\partial b_1}{\partial t} = k_1^f c_1 (b_1^{max} - b_1) - k_1^r b_1 \quad (6)$$

$$\frac{\partial b_2}{\partial t} = k_2^f c_1 (b_2^{max} - b_2) - k_2^r b_2 \quad (7)$$

where c_1 is the concentration of a drug transported in the arterial wall b_1 and b_2 denote non-specifically and specifically bound drug, respectively, k_i^f, k_i^r, b_i^{max} are constant parameters related to the binding kinetics, $\mathcal{D}_1$ is diffusion coefficient, given, in this work, by an anisotropic tensor.

The tensor $\mathcal{D}_1$ is constructed from the principal directions α_i and the principal values λ_i, as: $\mathcal{D}_1 = P\Lambda P^{-1}$ where Λ is the diagonal matrix of the principal values, and P is the block matrix of column vectors α_i, given by $P = (\alpha_1 \alpha_2)$. The direction α_1 is perpendicular to the direction of the fibers of the arterial tissue and therefore it is associated to a smaller diffusion principal value λ_1, while the direction α_2 is tangent to the direction of the arterial fibers, hence associated to a large diffusion principal value λ_2. Values of λ_1 and λ_2 are taken from the radial and axial diffusion coefficients reported in the literature (Lucena *et al.* (2018)). To obtain an approximation of the direction perpendicular to the fibers (α_1) we employ the gradient of a marker function d

$$\alpha_1 = \nabla d \qquad \text{and} \qquad \nabla^2 d = 0, \quad (8)$$

where d is either taken as the shortest euclidean distance between the point and all the discrete points on the artery internal surface or computed for every mesh point as the solution of the above equation. Subsequently, the direction α_2 is constructed employing orthogonality.

The computed distance d field is shown in Fig. 2(a), and the principal directions field in the right half of the domain is shown in Fig. 2(b). The permeability in the polymer coating, P_{D0}, is considered to be very small, but finite. The endothelium lamina, where present, is modeled as a no-flow boundary. The boundary conditions on drug in the denuded endothelium is $c_1 = 0$, between polymer and blood, i.e., on interface Γ_1 is $c_0 = 0$, (see Fig. 1(a)). We assume periodic conditions at the side boundaries. The mass flux is established across the interface and the drug starts to be transferred to the adjacent release medium.

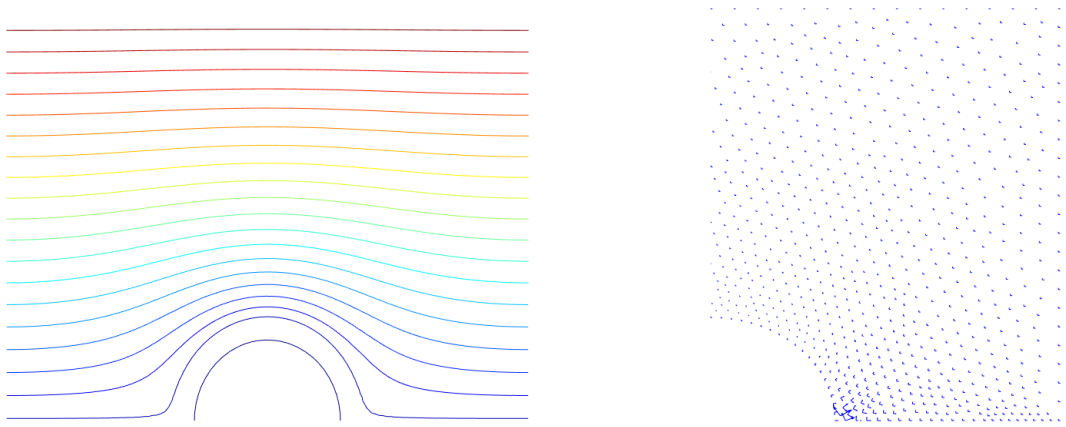

(a) (b)

Figure 2: (a) Distance field d using the laplacian approach. (b) Principal directions field, in the right half of the domain.

2.1 Evaluation of the flux and of the total mass transferred from the stent

The mass flux is established across the interface and the drug starts to be transferred to the adjacent release medium. The instantaneous flux is given by:

$$\varphi_i(t) = \int_{\Gamma_i} \mathbf{n} \cdot \mathcal{D}_0 \nabla c_0(t) d\Gamma, \quad \text{with} \quad i = 1, 2, \quad (9)$$

where $i = 1$ refers to the lumen interface, $i = 2$ refers to the arterial wall, and $\mathbf{n}$ is the surface normal. $d\Gamma = 2\pi r ds$ and the mass flux (integral) is given by:

$$\Phi_i = \int_0^t \varphi_i(t) dt, \tag{10}$$

where t is the time.

A verification of the mass balance of the simulation can be performed by comparing the total mass that leaves the stent and enters the adjacent media, divided by the volume

$$C_\Phi(t) = \frac{\Phi_1(t) + \Phi_2(t)}{V}. \tag{11}$$

The governing equations in bidimensional axisymmetric coordinates are solved on an unstructured triangular mesh, using linear base functions and the Galerkin Finite Element Method (see Lucena *et al.*, 2018). The dimensional parameters employed in the simulations are shown in Tab. 1.

Table 1: Dimensional parameters used in the simulations. Values of $r_0, r_{max} - r_0, d_s, L_s, L_p, L_z, p_{wall}, \mu, D_0, P_{D1}, \phi_1, D_{1r}, D_{1z}$ were obtained from Bozsak *et al.* (2014). Values of $\beta_0, B_0, S_0, k_1^f, k_1^r, b_1^{max}, k_2^f, k_2^r, b_2^{max}$ were obtained from McGinty and Pontrelli (2016)

Parameter		Simulated value
r_0	lumen radius	1.5×10^{-3}m
$r_{max} - r_0$	arterial wall thickness	5.0×10^{-4}m
d_s	stent strut diameter	2.5×10^{-4}m
L_s	denuded endothelium	1.5×10^{-4}m
L_p	polymer thickness	5.0×10^{-5}m
L_z	domain length	7.0×10^{-4}m
p_{wall}	lumen overpressure	9.31×10^3 Pa
μ	fluid viscosity	7.2×10^{-4} Pa
dt	simulation time step	100s
t_{end}	time of simulation	20 days
	Polymer layer	
P_{D0}	permeability	2.78×10^{-21}m^2
ϕ_0	porosity	0.29
β_0	dissolution rate	1.0×10^{-4}(mol m^{-3})$^{-2/3}$ s^{-1}
B_0	initial drug eluting	100 mol m^{-3}
S_0	drug solubility	$B_0/10$ mol m^{-3}
$\mathcal{D}_0$	fast diffusion coefficient	1.0×10^{-14}m^2 s^{-1}
	Arterial wall	
P_{D1}	permeability	2.0×10^{-18}m^2
ϕ_1	porosity	0.29
$\mathcal{D}_{1r} = \lambda_1$	radial diffusion coefficient	7×10^{-12}m^2 s^{-1}
$\mathcal{D}_{1z} = \lambda_2$	axial diffusion coefficient	4×10^{-11}m^2 s^{-1}
k_1^f		2 (mol m^{-3} s)$^{-1}$
k_1^r		5.2×10^{-3} s^{-1}
b_1^{max}		3.63×10^{-1} mol m^{-3}
k_2^f		800 (mol m^{-3} s)$^{-1}$
k_2^r		$1.6 \times 10^{-4} s^{-1}$
b_2^{max}		3.3×10^{-3} mol m^{-3}

3. COMPUTATIONAL RESULTS AND DISCUSSION

Pressure and velocity fields are assumed as constant along the simulation of the sirolimus transport, and, numerically, these distributions do not change with the choice of the approach (euclidean or laplacian distance) that we use to calculate the principal directions. The pressure and velocity fields are shown in Fig. 3.

A two dimensional renderization of the velocity field, shown in Fig. 3(b), presents higher velocities between the endothelium lamina and at the denuded endothelium, due to the prescribed boundary conditions for the velocity. The maximum velocity magnitude observed from the simulations is $\mathbf{u}_{\max} = 6.2718 \times 10^{-7}$ m·s^{-1}.

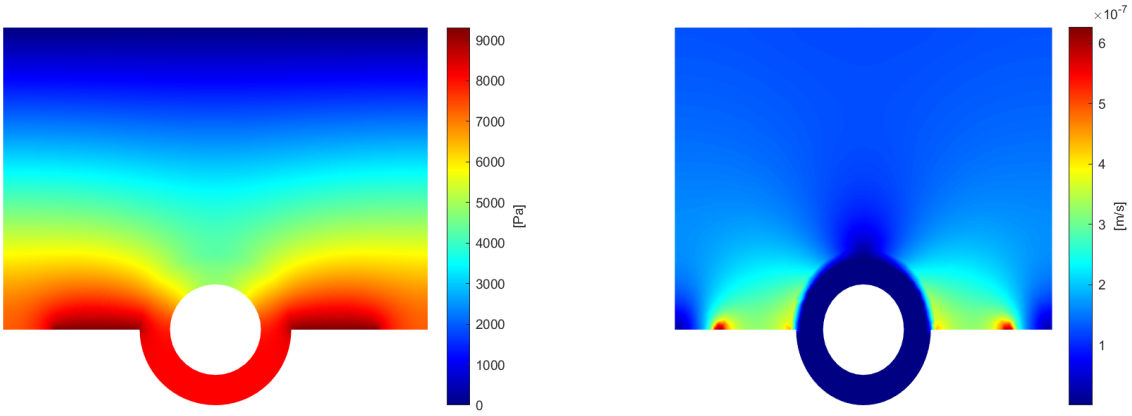

(a) (b)

Figure 3: (a) Pressure field obtained by the solution of Darcy's Law (Eq. (2)) and (b) Magnitude of velocity computed from Eq. 1, with $\mathbf{u}_{\max} = 6.2718 \times 10^{-7}$ m·s^{-1}

3.1 Fast release polymer - Orthotropic x Anisotropic

According to Lucena *et al.* (2018), the simulation starts with all the sirolimus in solid form in the polymer layer, with concentration B_0, and null concentration elsewhere. The solid sirolimus gradually dissolves in the polymer layer and diffuses to the porous artery wall, where it is convected-diffused-bound (see Figs. 4, 5 and 6).

Figure 4 shows the results of dissolved sirolimus concentration, c_0, for fast release in the polymer layer at $t = 15$ days for the orthotropic and the anisotropic tensors, respectively. We can see that the behavior is almost equal in both tensors, once the main difference is given in the arterial wall.

The results of sirolimus concentration of drug, c_1, being transported across the arterial wall at $t = 2$ and $t = 15$ days are shown is Figs. 5 and 6, respectively. Figures 5(a) and 6(a) show the results for orthotropic tensor and Figs. 5(b) and 6(b) show the results obtained to the anisotropic tensor. We can observe that for the anisotropic medium there is a more dissolution of the concentration, as well the behavior above the polymer layer is more spread around the ring in relation to the orthotropic medium, at times $t = 2$ and $t = 15$ days.

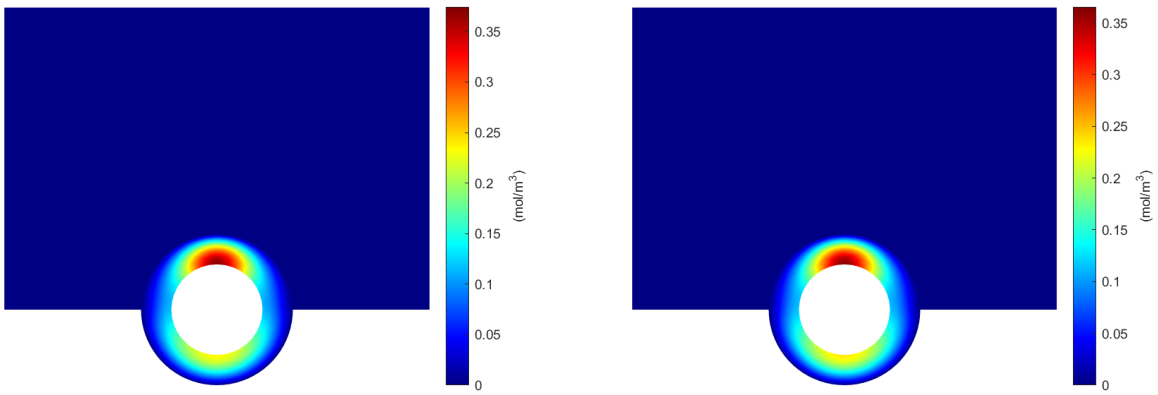

(a) (b)

Figure 4: Results of sirolimus concentration for fast release polymer at $t = 15$ days for (a) orthotropic and (b) anisotropic tensors, respectively. Dissolved concentration (c_0) in the polymer layer.

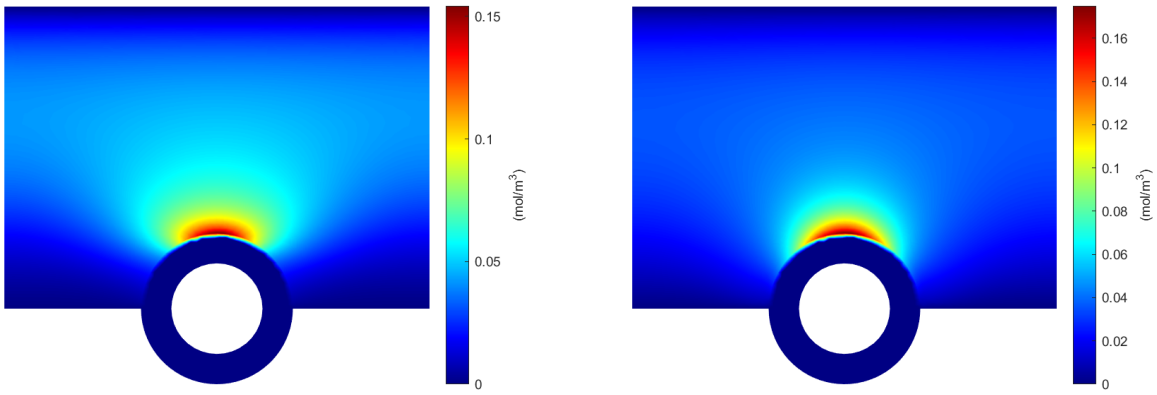

(a) (b)

Figure 5: Results of the sirolimus concentration field for fast release of the polymer at $t = 2$ days. (a) orthotropic tensor; (b) anisotropic tensor, for a concentration of drug (c_1) being transported across the arterial wall.

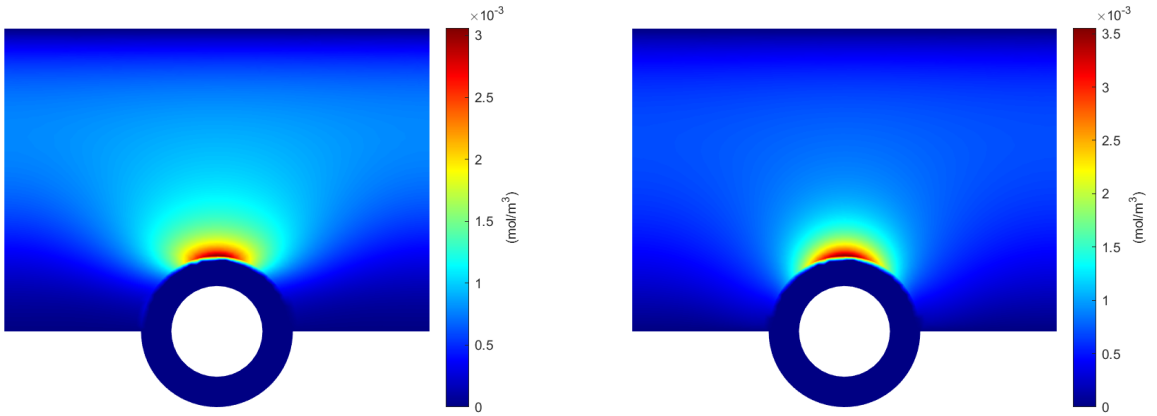

(a) (b)

Figure 6: Results of the sirolimus concentration field for fast release of the polymer at $t = 15$ days. (a) orthotropic tensor; (b) anisotropic tensor, for a concentration of drug (c_1) being transported across the arterial wall.

The aim of this study is to evaluate the effect of the anisotropic diffusion tensor using the laplacian approach for evaluate the principal directions compared to the results obtained by Lucena *et al.* (2018) and Frazzoli *et al.* (2018) where the orthogonal tensor was adopted.

We plot the difference between the concentration field, c_1, for the cases as shown in Fig. 7. A more clear difference appears at the upper region of the stent, which is in contact with the arterial wall due to the effect induced by the principal directions. This effect does not exist whenever the flattening of the fibers of the arterial wall, caused by the stent.

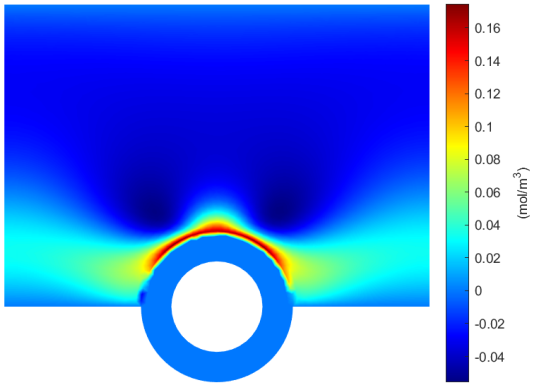

Figure 7: Two dimensional concentration difference between the orthotropic and the anisotropic mediums at $t = 15$ days, using the principal directions evaluated with the laplacian, for the case of fast release of the polymer.

The procedure adopted to quantify the evolution of the concentration of the distribution, we check the concentration at two positions along of an horizontal line (in position $r = 1.69 \times 10^{-3}$ m) and along an inclined line with angle of inclination $\theta = 45°$ (from $r = 1.5 \times 10^{-3} m$ and $z = 4.75 \times 10^{-4}$m). Figure 8 shows the the result for the concentration at the horizontal line and the difference between these results, respectively.

Figure 9 shows the concentration evaluated at the inclined line and the difference between both curves. One can see a higher concentration in the orthotropic medium at this chosen horizontal position. However, the anisotropic medium presents a higher concentration at that inclined line. In both cases, the observed concentration difference is of order of 10^{-4}.

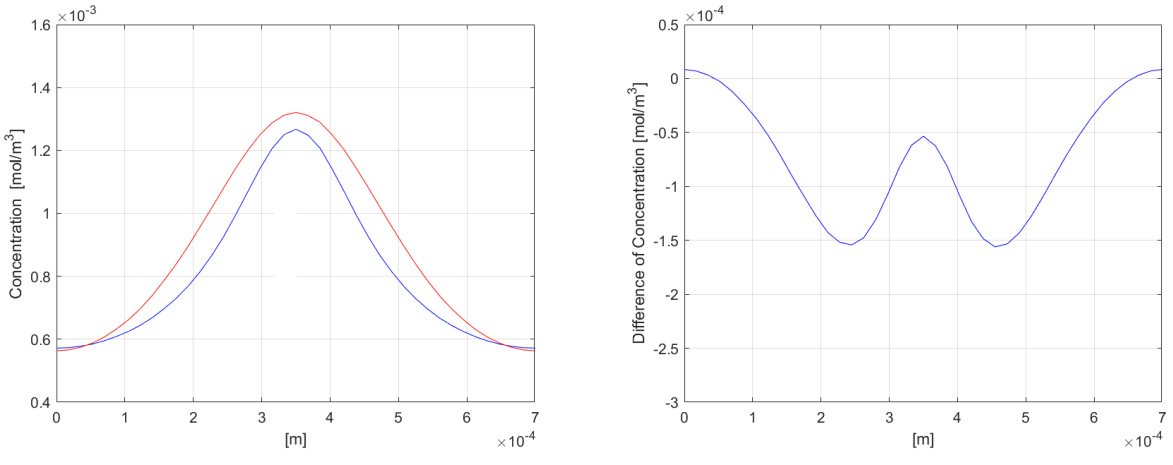

(a) (b)

Figure 8: Concentration field evaluated at the horizontal line at $t = 15$ days, for anisotropic and orthotropic mediums, and with principal distances evaluated with the laplacian. (a) Concentration plot for both approaches. In red: curve for orthotropic porous media. In blue: curve for anisotropic porous media. (b) Plot of the difference between the two curves.

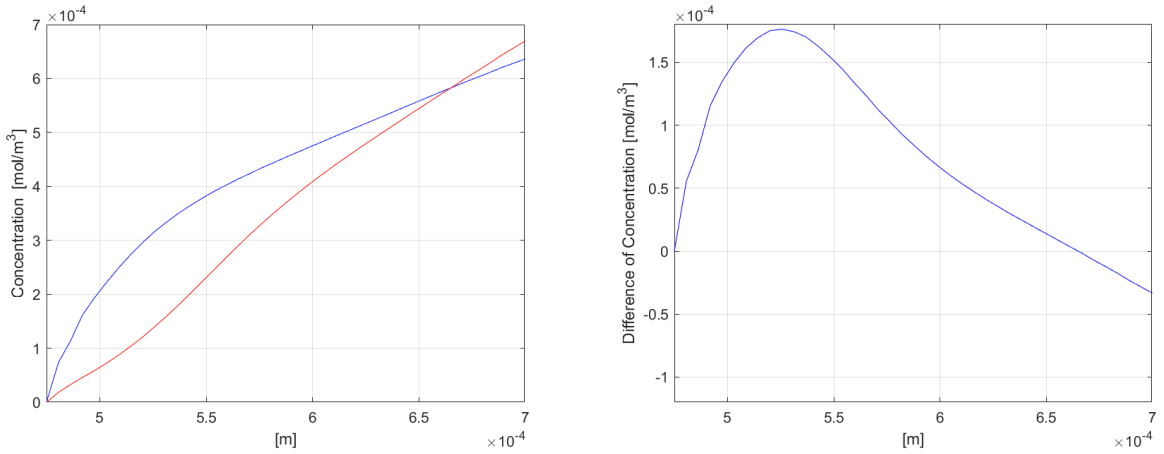

(a) (b)

Figure 9: Concentration field evaluated at the inclined line ($\theta = 45°$) at $t = 15$ days, for anisotropic mediums, and orthotropic, with principal distances evaluated with the laplacian. (a) Concentration plot obtained with the two approaches. In blue curve: anisotropic porous media. In red: curve is in orthotropic porous media. (b) Plot of the difference between both curves.

The total amount of mass, in mols, of the drug, transferred to the arterial wall and the lumen is estimated using Eq. 11. Fig. 10 (a) shows this total amount of transferred mass, obtained with the two models using the two mediums employed, for orthotropic and anisotropic mediums. From Fig. 10(b), we note that differences of the results obtained with one model and with the other one is of order of 10^{-3}.

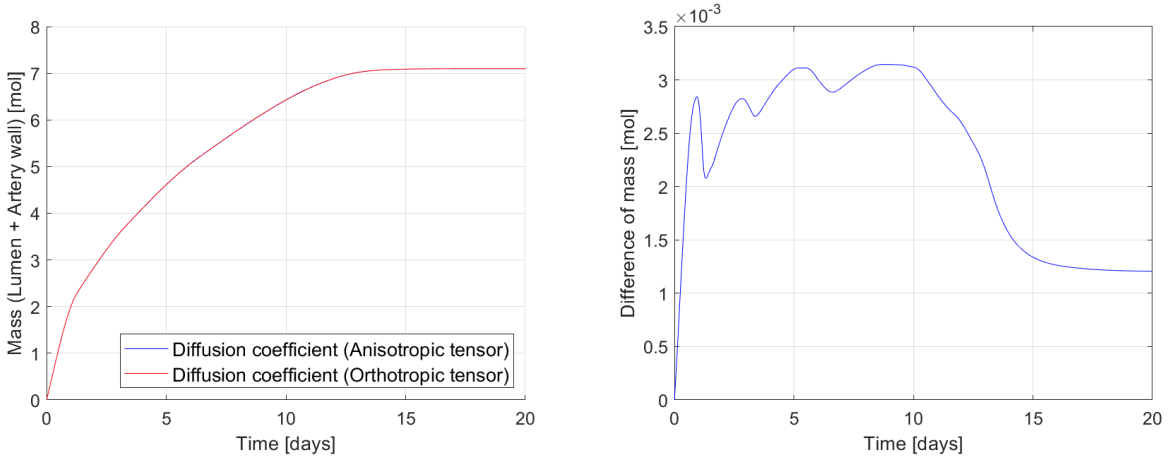

(a) (b)

Figure 10: (a) The total amount of mass, in mols, of the drug, transferred to the arterial wall and the lumen is estimated using Eq. 11, orthotropic and anisotropic mediums, respectively. (b) Difference of the total mass between the two mediums.

4. CONCLUSIONS

The simulations of the transport through a polymer layer and a porous arterial wall with binding in drug-eluting stent is performed. We consider the model of dissolution, transport and binding of sirolimus on an axisymmetric domain representing the polymer coating layer and the porous artery wall in the vicinity of a stent strut. We employ the FEM on an unstructured mesh to discretise the governing equations.

In this work, a new anisotropic model for the diffusion tensor in the artery wall that takes into account the realignment of the principal directions of the diffusion tensor due to the introduction of the stent, employing an algebraic model to define the principal directions, was presented. Results of simulations with the new model were compared to results obtained with a previous orthotropic model (Frazzoli *et al.* (2018)), we can conclude that the new approach corrects the behaviour in the corner between the stent and the arterial wall in the horizontal direction.

5. ACKNOWLEDGEMENTS

The authors would like to acknowledge financial support from FAPERJ, CAPES, CNPq, and the University of Glasgow EPSRC GCF ISF fund.

6. REFERENCES

Bozsak, F., Chomaz, J. and Barakat, A., 2014. "Modelling the transport drugs of eluted from stents: physical phenomena driving drug distribution in the arterial wall". *Biomech Model Mechanobiol*, Vol. 13, pp. 327–347.

Chisari, A., Pistritto, A., Piccolo, R., Manna, A.L. and Danzi, G., 2016. "The ultimaster biodegradable-polymer sirolimus-eluting stent: An updated review of clinical evidence". *Int. J. Mol. Sci.*, Vol. 17(9), p. 1490.

Frazzoli, F., Lucena, R., Mangiavacchi, N., Pontes, J., Anjos, G. and McGinty, S., 2018. "Anisotropic transport through polymer layer and porous arterial wall with binding in drug-eluting stents using the FEM". In *17th Brazilian Congress of Thermal Sciences and Engineering*.

Lucena, R., Mangiavacchi, N., Pontes, J., Anjos, G. and McGinty, S., 2018. "On the transport through polymer layer and porous arterial wall in drug-eluting stents". *Journal of the Brazilian Society of Mechanical Sciences and Engineering*, Vol. 40, No. 572.

McGinty, S. and Pontrelli, G., 2016. "On the role of specific drug binding in modelling arterial eluting stents". *J Math Chem*, Vol. 54, pp. 967–976.

7. RESPONSIBILITY NOTICE

The authors are the only responsible for the printed material included in this paper.